

# Testing of Membrane Space Structure Shape Control Using Genetic Algorithm

Fujun Peng,\* Yan-Ru Hu, and Alfred Ng

*Directorate of Spacecraft Engineering, Canadian Space Agency,  
St.-Hubert, Quebec J3Y 8Y9, Canada*

DOI: 10.2514/1.16127

**This paper investigates the application of the genetic algorithm in active control of inflatable structures. The algorithm is used to search for the optimal tensions, which minimize membrane wrinkles. A genetic algorithm-based control system is developed using MATLAB, LabView, and Automation Manager. The control system is tested on a 200 × 300 mm rectangular Kapton membrane pulled by three tensions along each edge. Different tension combinations are exerted onto the membrane through SMA actuators. All tensions are calculated through the strains of a thin aluminum strip installed in the tension links. A vision system is developed to measure the membrane flatness under different tension combinations. Testing results show that the genetic algorithm works very well in finding the optimal tensions.**

## Nomenclature

$I(t)$	=	electrical current at time $t$
$I_c$	=	constant electrical current
$M$	=	$4 \times 3$ camera calibration matrix
$S(t)$	=	measured value of tension at time $t$
$S^*(t)$	=	required value of tension at time $t$
$U, V$	=	homogeneous coordinates (pixels)
$x, y, z$	=	3-D coordinates of observed points

## I. Introduction

**I**NFLATABLE structures have attracted much interest in the space community due to their unique advantages in achieving low mass and high packaging efficiency [1,2]. Their ultralightweight and small-volume properties in turn can potentially reduce the overall space program cost by reducing the launch vehicle size requirement. Inflatable structures can also reduce total system mass and the number of deployment mechanisms, thereby increasing system reliability. This type of structures has been envisioned for many space applications such as large telescopes, antennas, solar sails, sun shields, solar arrays, etc. [1–4].

We are currently working on an in-house research and development project in the development of a large surface area to mass ratio inflatable space structure with possible applications as a synthetic aperture radar antenna. The key components of this inflatable structure are inflatable tubes, membrane, and the links installed in between stretching the membrane (Fig. 1). It can be rolled into a small volume and fixed on a small satellite bus for launching. When the satellite arrives into orbit, the inflatable tubes are filled with gas and roll out, and the Kapton membrane will be deployed accordingly.

It is expected that the membrane will be subjected to flatness problems during its lifetime in orbit due to the thermal variation in space. A pure passive control method may not be sufficient to maintain the membrane flatness. Hence an active control system is proposed to adjust the tensions according to the thermal variation. The genetic algorithm is applied to search for the optimal tensions that minimize the membrane wrinkles. Actuators are installed in series with the links such that the tensions stretching the membrane can be adjusted. This paper presents some experimental results

obtained in controlling the flatness of a rectangular membrane. The membrane to be controlled is a 200 × 300 mm rectangular Kapton membrane, pulled by three tensions along each edge. Six shape memory alloy (SMA) wire actuators are used. Tests are performed in two cases: at room temperature with and without local thermal load. Experimental results show the genetic algorithm finds the optimal tension rapidly.

## II. Genetic Algorithm

The genetic algorithm (GA) is an optimization searching technique derived from the mechanics of natural selection and genetics. This mechanism has been mathematically shown to eventually “converge” to the best possible solution. Compared with traditional search and optimization procedures, the genetic algorithm is robust, and generally more straightforward to use. It is stochastic in nature, thus is capable of searching the entire solution space with more likelihood of finding the global optimum. The genetic algorithm is applicable to both linear and nonlinear systems where little or no a priori knowledge of the system is given [5,6].

To implement the search for the optimal tensions for the membrane, all the parameters (here, they are the amplitudes of tensions) to be optimized are first mapped (coded) into a chromosome. Each parameter corresponds to one particular portion of the chromosome. The block diagram is shown in Fig. 2. An initial population is randomly generated first, with each individual corresponding to a tension combination. Then the algorithm goes through “selection,” “crossover,” and “mutation,” and forms a new population. Generally speaking, the individuals in the new population perform better for the given task than the parent population. This procedure is repeated until some individuals are found that meet the requirement of the given task. After the optimal individuals are found, the optimal solution can be obtained by directly decoding the optimal individuals.

## III. Experimental Setup

The structure used for testing the genetic algorithm is shown in Fig. 3. The membrane is a 200 × 300 mm rectangular Kapton membrane, which is stressed by 12 discrete links installed between the membrane boundaries and the aluminum frame. A local thermal load source is placed under the membrane (not visible in Fig. 3). The flatness of the membrane is dependent on the local thermal load and the tension combinations. To realize active control, six shape memory alloy wire actuators are installed along the edge as a part of tension links. To monitor the values of tensions, strain gauges are glued onto small, thin aluminum strips, which are also parts of

Received 15 February 2005; revision received 13 October 2005; accepted for publication 4 January 2006. Copies of this paper may be made for personal or internal use, on condition that the copier pay the \$10.00 per-copy fee to the Copyright Clearance Center, Inc., 222 Rosewood Drive, Danvers, MA 01923; include the code \$10.00 in correspondence with the CCC.

\*E-mail: fujun.peng@space.gc.ca, pfj\_tj@yahoo.com. Member AIAA (corresponding author).

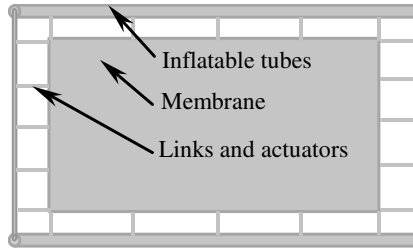


Fig. 1 Sketch of the inflatable structure.

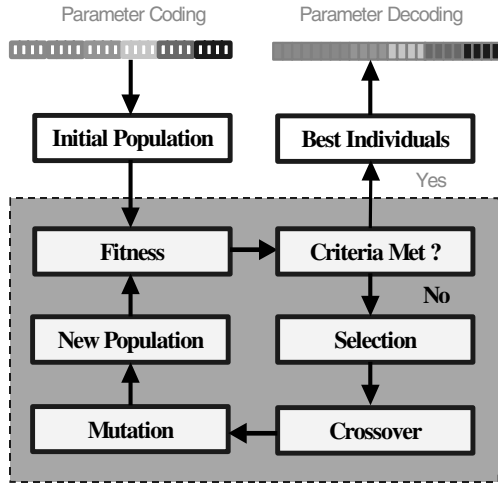


Fig. 2 Block diagram of the genetic algorithm.

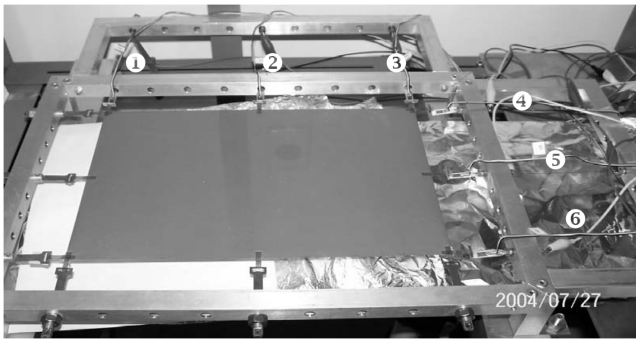


Fig. 3 Picture of the membrane structure used for experimental studies.

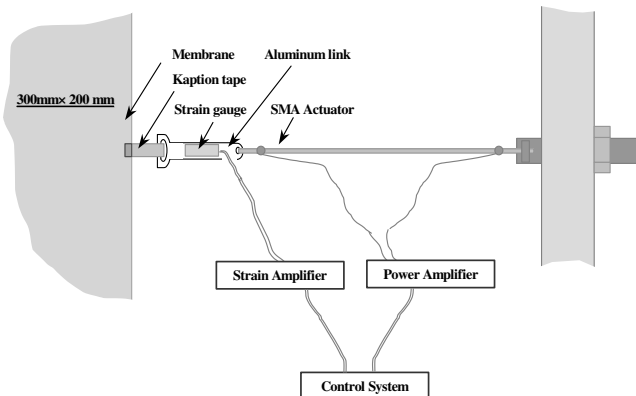


Fig. 4 Arrangement of actuators and sensors.

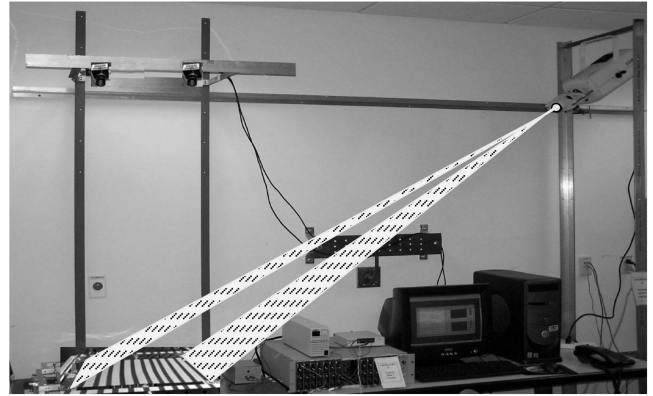


Fig. 5 Picture of the whole control system and setup.

tension links. The arrangement of the SMA actuator, strain gauge, and links is sketched in Fig. 4. These tension measurement elements are calibrated using a load cell before tests are performed. The capacity and precision are found to be on the order of 10 and 0.05 N, respectively. A vision system is used to measure the flatness of membrane. It employs a 1.3 megapixel digital camera. A projector shines lines on the membrane surface, and the vision system gives 3-D coordinates of the points selected on the line edges. In order for the vision system camera to see these lines clearly, a very thin coating is put on one side of the membrane. The vision system takes about 0.1 s to obtain 330 points 3-D coordinates, with the accuracy on the order of 0.05 mm (for a field of view of  $200 \times 300$  mm). The accuracy can be improved by using a higher resolution camera or applying a lens distortion compensation. Camera and projector calibrations are needed before performing flatness measurement. The whole setup including the vision system is shown in Fig. 5.

#### IV. Control System Implementation

The control system is implemented using LabView, MATLAB, and Automation Manager. LabView code controls parameter input, result display and data I/O including tension measurement and control signal output. MATLAB code implements the genetic algorithm. Automation Manager realizes the vision system. LabView code is the master, which coordinates the whole system functioning by using the ActiveX technique.

##### A. Genetic Algorithm Implementation

A key issue of implementing the genetic algorithm with hardware in the loop is the two-step fitness evaluation realization. For numerical simulation of the genetic algorithm as shown in Fig. 2, a new population production and its evaluation are completed within the same loop. Also, a new loop always starts with individual selection and ends at criteria judgment.

However, for experimental tests of the genetic algorithm with hardware in the loop, all individuals of a population have to be converted to control forces and output first, and then evaluated in the next loop according to the acquired flatness produced by them. Also, a new loop always starts with the fitness evaluation and ends at data I/O. The genetic algorithm initialization also requires two loops. The first loop generates an initial population and output the individuals in it. The tensions corresponding to these initial individuals are exerted to the real structure. The second initialization loop evaluates the fitness of the all the initial individuals, and then goes through "selection," "crossover," and "mutation" to generate a new population. The loops afterward go through the same procedure as the second loop, except they evaluate only part of the individuals because some best individuals of last loop are transferred to the new population in the present loop without any change. It should be noted that every individual has to be converted to control force combinations before it is output for tension control. The block

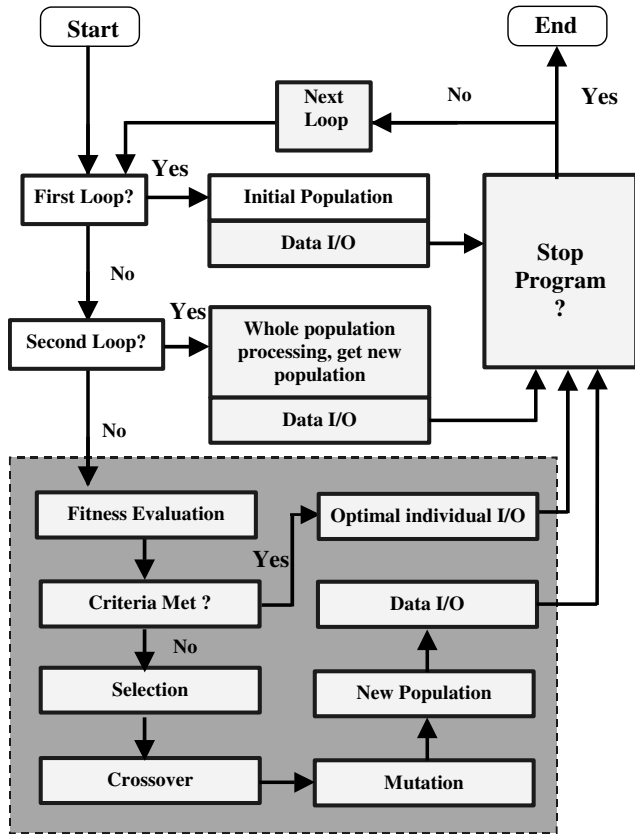


Fig. 6 Block diagram of the genetic algorithm implementation with hardware in the loop.

diagram of the genetic algorithm implementation with hardware in the loop is shown in Fig. 6, in which the second step of initialization is simply represented by only two rectangular blocks.

### B. SMA Actuator Controller Design

A challenge encountered here in using SMA for exerting tensions is that the SMA wire actuator cannot be used directly due to its poor stability and controllability. It is hard to identify a reliable relationship between its strain output and the electrical current input. Its low response speed is also a problem. For thin SMA wires, response speed is faster, but they are more sensitive to the air convection, and a steady strain output is not achievable even by applying a fixed current. So, a feedback controller is developed here to ensure that the required tension can be achieved with good accuracy. The current at time  $t$  is designed as

$$I(t) = \begin{cases} I_c, & \text{if } S^*(t) - S(t) \geq 0 \\ 0, & \text{if } S^*(t) - S(t) < 0 \end{cases} \quad (1)$$

where  $I_c$  has a relatively large value, but is not high enough to burn the SMA wire.  $S^*(t)$  is obtained from the genetic algorithm.  $S(t)$  is the practical value of the tension measured by the strain gauge at time  $t$ . This SMA wire control strategy is simple, absolutely stable, and no model is required. Test results show that with this control strategy, a SMA wire actuator can track square wave, ramp, and sinusoidal signals with very high accuracy: small overshoot and small steady error. Another advantage of this control strategy is that the SMA response speed is increased remarkably by using a high input current.

In the control system, this actuator controller is implemented by creating a LabView sub-VI. The actuator controller runs in the following order: When it is fed a control force combination (an individual) from the genetic algorithm, the sub-VI adjusts its outputs with very high rate and at the same time monitors the practical control force obtained. Within any iteration, if a measured control force is smaller than the required value, the corresponding channel is set to a

relatively high voltage, otherwise, the channel is set to zero voltage. After all the measured control forces experienced values greater than the required ones, the required tensions have been achieved.

### C. Vision System Implementation

Figure 7 shows the principle of the vision system. The camera is calibrated in 3-D world space, which allows a pixel in the camera plane to be mapped as a line (cone) radiating from the camera focal point in the world coordinate system. Similarly a light projector is used to project lines (planes) onto the membrane surface. These planes are also calibrated in the world coordinate space. The camera observes the points selected on the lines projected by the projector. The space between two adjacent lines can be adjusted by using a different gobo in front of the projector lens. The density of observed points chosen on a line is set in software. One observed point can be regarded as the intersection of the corresponding light plane and the associated radiating lines from the camera. The 3-D coordinates of any point can be calculated by solving the equations of the corresponding light plane and radiating line. After the 3-D coordinates of all selected points are obtained, the membrane flatness then becomes achievable by calculating the RMS error of these points. This could be realized by solving an eigenvalue problem, and the RMS error is the square root of its smallest eigenvalue divided by the total number of points.

The camera calibration involves a small rig that set a plate at two different heights. A target pattern (in our case it is an array of dots of known spacing) is observed at two heights. These dots are observed by the camera and the mathematics can be written as (in homogeneous units)

$$[x, y, z] \left( \begin{bmatrix} M(1, 1) \\ M(2, 1) \\ M(3, 1) \end{bmatrix} - U \begin{bmatrix} M(1, 3) \\ M(2, 3) \\ M(3, 3) \end{bmatrix} \right) = UM(4, 3) - M(4, 1) \quad (2)$$

$$[x, y, z] \left( \begin{bmatrix} M(1, 2) \\ M(2, 2) \\ M(3, 2) \end{bmatrix} - V \begin{bmatrix} M(1, 3) \\ M(2, 3) \\ M(3, 3) \end{bmatrix} \right) = VM(4, 3) - M(4, 2) \quad (3)$$

Substituting the target coordinates  $x_i$ ,  $y_i$ , and  $z_i$  ( $i = 1, \dots, n$ , where  $n$  is the total number of calibration targets) and corresponding  $U_i$  and  $V_i$  ( $i = 1, \dots, n$ ) into Eqs. (2) and (3) and applying a best fit solution, the camera calibration matrix  $M$  can be obtained.

The software is implemented using Automation Manager Language, which is a graphical programming language developed by a company. The camera and light plane calibrations, point density selected on lines, and 3-D coordinate computations are all realized in this language. The software runs as a separate module under the coordination of the control system.

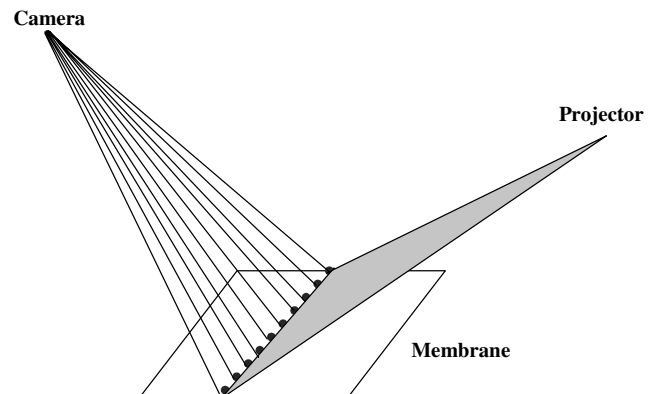


Fig. 7 Principle of the vision system implementation.

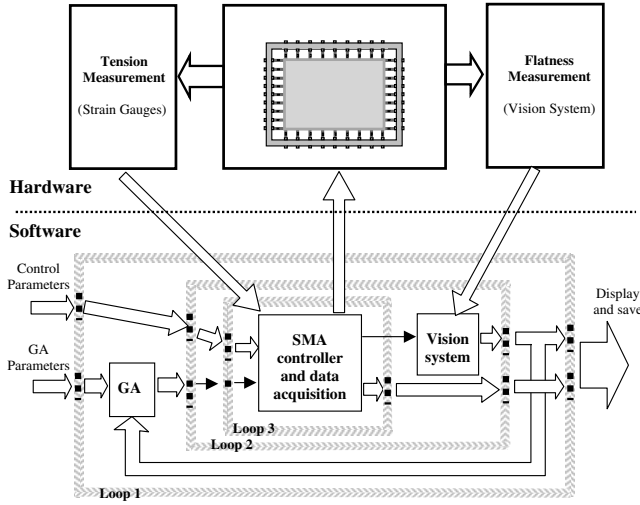


Fig. 8 Block diagram of the control system implementation.

#### D. Control System Integration

The implementation of the whole control system is illustrated in Fig. 8. To complete one generation, Loop 1 runs only one cycle. The cycle number of Loop 2 running is the total number of new individuals in every population. Loop 3 runs much more cycles than Loop 2 and the specific number is always changing depending on the largest difference of the tension corresponding to the same actuator in two adjacent generations. If the difference is large, the actuator then needs more time to change its status from the parent individual to the new one, and thus more cycles are needed.

The control system can be terminated by two ways. One is that it stops automatically after a number of generations are completed. This total number should be carefully determined to ensure the optimal tension combinations can be found before the control system stops. The advantage of this method is its simplicity and ease of implementation. Its disadvantage is that the obtained optimal tension combination cannot be held for a relatively long period of time, and consequently the membrane status cannot be maintained for observation. When the genetic algorithm is searching for the optimal tensions, each tension combination is held less than 1 s. After the control system completes the predetermined number of generations, the power is removed right away from all the actuators. The other termination method is to set a required level of membrane flatness. When the control system finds an optimal tension combination that produces a better membrane flatness than the required value, the genetic algorithm stops the searching process. Then Loop 2 will not accept other individuals, but output the obtained optimal control force for a relatively long time. This will allow the membrane remaining at the optimal state for observation. The length of the waiting time can be set through the control system graphical user interface. During this period of time, the genetic algorithm is waiting for the end of the actuator controller running, and the whole program stops as soon as the assigned time runs out.

### V. Experiments and Results

The experiment is firstly performed at room temperature without local thermal load. Upper and lower limits of tensions are set at 4.00 and 1.33 N, respectively. There are eight individuals in one population, and four of them are updated at one time. Gray coding, stochastic universal sampling, multipoint crossover and discrete mutation are used in GA. The experiments are performed 20 times and each time 20 generations are tested. It is found that the control system finds the optimal tension combination very quickly, and the corresponding rms error of the membrane is reduced from around 0.22 mm to less than 0.05 mm. Figure 9 shows typical statuses of the membrane without and with control, and Fig. 10 shows the 20 best tension combinations obtained from the 20 experiments, respectively. Each column corresponds to one optimal

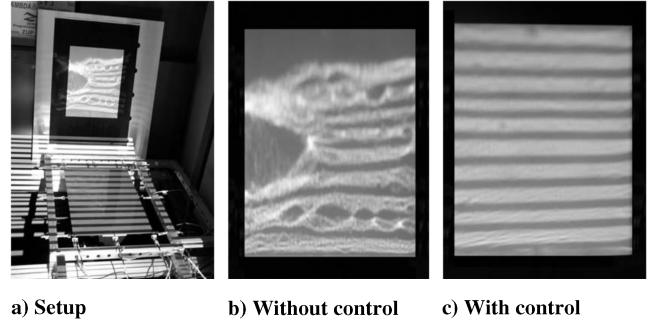


Fig. 9 Observation of membrane flatness, typical status of membrane before and after control.

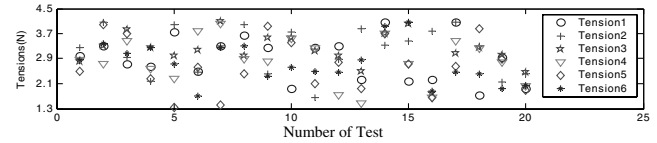


Fig. 10 Twenty optimal tension combinations obtained without local thermal load.

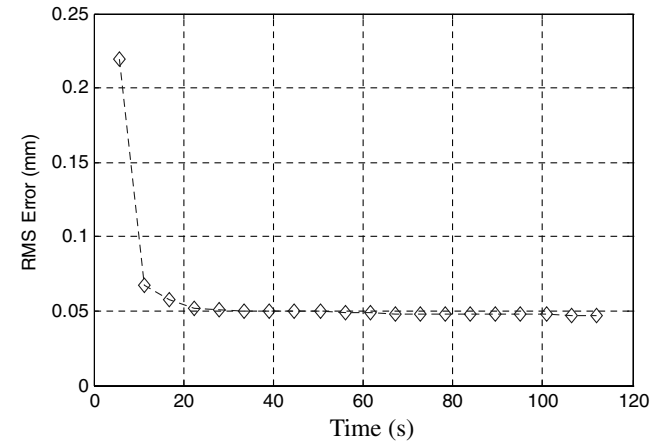


Fig. 11 Average of flatness convergences of 20 generations of optimal tension combinations.

tension combination, which includes six tensions. Figure 9a is an observation system specifically designed for demonstration, in which the reflected image is a direct judgment of the membrane flatness. If the membrane is flat, the lines shined on the membrane will be straight and the reflected image will be straight lines too. But if there is any wrinkle generated, the distortion will be amplified on the reflected image. The comparison of Figs. 9b and 9c shows clearly that the membrane flatness is improved significantly. But taking a look at Fig. 10, one may be confused by the seemingly irregular distribution of the optimal tension combinations. In fact, for a membrane with boundary conditions similar to this setup, the optimal tension combination is not unique. There exists a region in a six-dimensional data space, in which all the tension combinations can improve the membrane flatness. The size of this region becomes smaller if complicated local thermal loads are applied and the required flatness level is stringent. In our case, the test is performed at room temperature and no local thermal load is applied, so the optimal region should be quite large. That is why the obtained 20 optimal tension combinations seem irregular. Figure 11 shows the average of rms error convergences of these 20 tests, in which we can see the membrane flatness is improved greatly. To further clarify and verify the above explanation, the last optimal tension combination (1.60, 2.14, 2.18, 1.69, 1.56, and 1.74 N) is exerted to the membrane, but

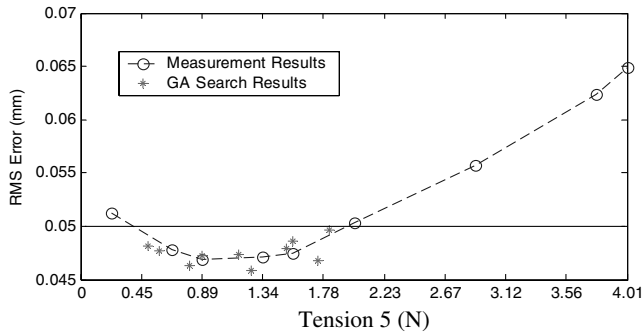


Fig. 12 Test results under different values of tension 5.

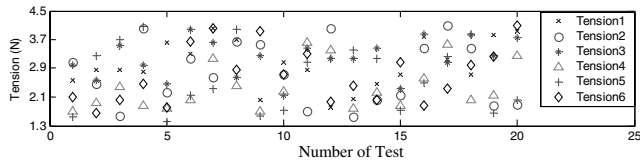


Fig. 13 Twenty optimal tension combinations obtained with local thermal load applied.

tension 5 is changed from 0.27 to 4.00 N, and corresponding membrane flatness is recorded. The measurement results are shown in Fig. 12. It is seen that the best membrane flatness can be achieved when tension 5 takes values between 0.89 and 1.34 N. If the required flatness level is 0.05 mm, the corresponding optimal tension region becomes larger, i.e., between around 0.4 and 1.96 N.

To further verify the effectiveness of the genetic algorithm, more tests are conducted with the upper and lower tension limits fixed at the last optimal tension combination, except that tension 5 is set adjustable between 0.22 and 4.00 N. Ten tests are performed with the required flatness level set as 0.05 mm, and each time the genetic algorithm tries to search the optimal value for tension 5. For comparison purpose, the obtained values of tension 5 and the corresponding rms errors are also put in Fig. 12. Clearly all the obtained values of tension 5 fall in the optimal region between 0.4 and 1.96 N. This result demonstrates that the genetic algorithm is effective in searching optimal tensions.

Tests are also performed with local thermal load applied to the membrane. A heater with a 75-mm-diam flat head is placed 5 mm under the membrane. It is located carefully to keep a proper distance from the strain gauges, such that no apparent effect happens to the tension measurement. This local thermal source makes the temperature distribution on the membrane neither uniform nor symmetric. Also, the local thermal load applied to the membrane produces dynamic wrinkles, which is fluctuating all the time. The position of the heater is fixed and its temperature remains unchanged at around 200°C. The control parameters and the genetic algorithm parameters are set the same as the case without local thermal load. The obtained 20 optimal tension combinations are shown in Fig. 13, and the average of the corresponding rms error convergences is shown in Fig. 14. Again the obtained 20 optimal tension combinations seem irregular, whereas the average of rms error convergences shows the genetic algorithm is still effective. Similar to the case without thermal load, the last optimal tension combination (3.83, 1.56, 3.60, 3.07, 1.69, and 4.00 N) is exerted to the membrane and then tension 2 is changed from 0.45 to 4.0 N, whereas other tensions remain unchanged. The obtained flatness values are shown in Fig. 15. It can be seen that better flatness is achieved when tension 2 becomes larger from 0.45 to 4.0 N. If the required flatness level is 0.05 mm, the corresponding optimal region is around between 1.25 and 4.0 N.

Tests are performed again with the upper and lower tension limits fixed at the last optimal tension combination, except that tension 2 is set adjustable between 0.22 and 4.0 N. Ten tests are performed with the required flatness level set as 0.05 mm. The obtained values of tension 2 and rms errors are also illustrated in Fig. 15. Obviously all

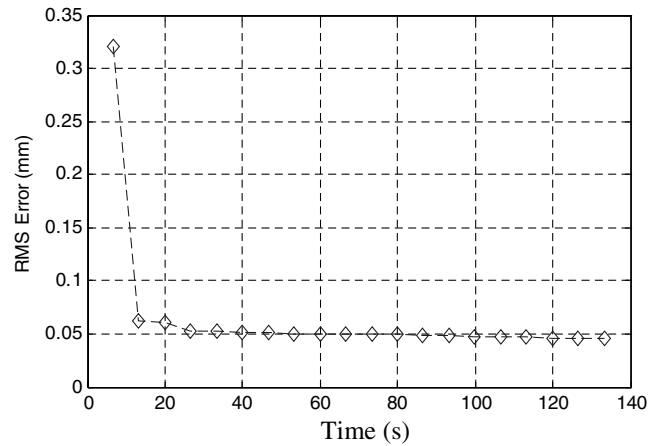


Fig. 14 Time histories of optimal flatness under thermal load.

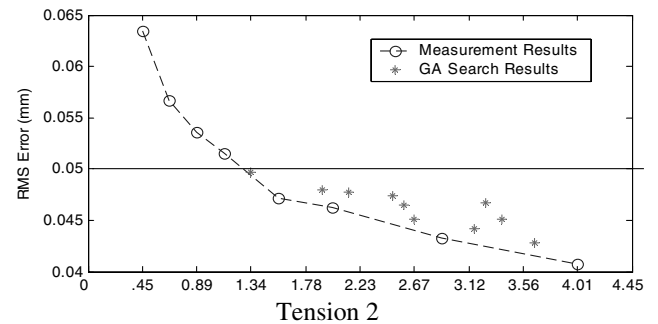


Fig. 15 Test results under different values of tension 2 with thermal load applied.

the obtained optimal values of tension 2 fall in the expected region, which demonstrates the effectiveness of the genetic algorithm in searching for the optimal tensions. Whereas the trends agree between the measurement and GA search, the amplitudes do not agree closely. This may be due to the limitation of the vision system accuracy.

## VI. Conclusion

This paper investigates the active control of inflatable membrane structure using the genetic algorithm. A control system is developed based on LabView, MATLAB, and Automation Manager. A feedback controller is developed to control SMA wire actuators. A vision system is implemented and used to measure membrane flatness. Tests are performed on a setup with a 200 × 300 mm Kapton membrane at room temperature with and without local thermal load, respectively. The results demonstrate the effectiveness of the genetic algorithm in searching for the optimal tensions. Further studies are being conducted on the application of this GA-based control system to membrane structures with flexible frames.

## References

- [1] Chmielewski, A. B., "Overview of Gossamer Structures," *Gossamer Spacecraft: Membrane and Inflatable Structures Technology for Space Applications*, edited by C. H. M. Jenkins, Vol. 191, Progress in Astronautics and Aeronautics, AIAA, Reston, VA, 2001, pp. 1–33.
- [2] Cadogan, D., and Grahne, M., "Inflatable Space Structures: A New Paradigm for Space Structure Design," IAF Paper IAF-98-1.1.02, Sept. 1998.
- [3] Lin, J. K. H., and Cadogan, D. P., "An Inflatable Microstrip Reflectarray Concept for Ka-Band Applications," AIAA Paper 2000-1831, April 2000.
- [4] Darooka, D. K., and Jensen, D. W., "Advanced Space Structure Concepts and Their Development," AIAA Paper 2001-1257, April 2001.

- [5] Hansen, C. H., Simpson, M. T., and Cazzolato, B. S., "Genetic Algorithms for Active Sound and Vibration Control," *Inter-Active'99 IEE International On-line Conference on Active Control of Sound and Vibration* [online proceedings], Univ. of Adelaide, South Australia, <http://www.mecheng.adelaide.edu.au/anvc/abstract.php?abstract=55> [cited April 2002].
- [6] Chambers, L. (ed.), *The Practical Handbook of Genetic Algorithms: Applications*, 2nd ed., Chapman & Hall/CRC, Boca Raton, FL, 2000, Chap. 1.

G. Agnes  
Associate Editor